

1 **Precipitation and synoptic regime in two extreme years**
2 **2009 and 2010 at Dome C, Antarctica – implications for ice**
3 **core interpretation**

4
5
6 **E. Schlosser^{1,2}, B. Stenni³, M. Valt⁴, A. Cagnati⁴, J. G. Powers⁵, K. W. Manning⁵,**
7 **M. Raphael⁶, and M. G. Duda⁵**

8
9 [1] {Inst. of Atmospheric and Cryospheric Sciences, University of Innsbruck,
10 Innsbruck, Austria}

11 [2] {Austrian Polar Research Institute, Vienna, Austria}

12 [3] {University of Venice, Venice, Italy}

13 [4] {Avalanche Service Arabba, Italy}

14 [5] {National Center for Atmospheric Research, Boulder, CO, USA}

15 [6] {Department of Geography, University of California, Los Angeles, California,
16 USA}

17
18
19
20
21 submitted to: Atmospheric Chemistry and Physics

22 18 September 2015

23 revised version for ACPD 13 October 2015

24 revised version after review 10 February 2016

25 re-revised version March 23th 2016

26
27
28 Correspondence to: E. Schlosser (Elisabeth.Schlosser@uibk.ac.at)

29

30

31 **Abstract**

32

33 At the East Antarctic deep ice core drilling site Dome C, daily precipitation measurements
34 have been initiated in 2006 and are being continued until today. The amounts and stable
35 isotope ratios of the precipitation samples as well as crystal types are determined. Within the
36 measuring period, the two years 2009 and 2010 showed striking contrasting temperature and
37 precipitation anomalies, particularly in the winter seasons. The reasons for these anomalies
38 are analysed using data from the mesoscale atmospheric model WRF (Weather Research and
39 Forecasting Model) run under the Antarctic Mesoscale Prediction System (AMPS). 2009 was
40 relatively warm and moist due to frequent warm air intrusions connected to amplification of
41 Rossby waves in the circumpolar westerlies, whereas the winter of 2010 was extremely dry
42 and cold. It is shown that while in 2010 a strong zonal atmospheric flow was dominant, in
43 2009 an enhanced meridional flow prevailed, which increased the meridional transport of heat
44 and moisture onto the East Antarctic plateau and led to a number of high-
45 precipitation/warming events at Dome C. This was also evident in a positive (negative) SAM
46 (Southern Annular Mode) index and a negative (positive) ZW3 (Zonal Wave number three)
47 index during the winter months of 2010 (2009). Changes in the frequency or seasonality of
48 such event-type precipitation can lead to a strong bias in the air temperature derived from
49 stable water isotopes in ice cores.

50

51

52 **1 Introduction**

53

54 Although Antarctic precipitation has been studied for approximately half a century (see e.g.
55 Bromwich, 1988), a number of open questions remain. There are two key motivations for
56 studying Antarctic precipitation. The first is that precipitation/snowfall is the most important
57 positive component of the mass balance of Antarctica. This is receiving increasing attention in
58 discussions of climate change since the mass balance response to global warming can
59 considerably influence sea level change. A possible increase of precipitation in a future
60 climate due to higher air temperatures and therefore increased saturation vapour pressure
61 would mean storage of larger amounts of water in the Antarctic ice sheet, thus mitigating sea

62 level rise (Church et al., 2013). So far, the expected increase in precipitation has not been
63 found in the measurements (e.g. Monaghan et al., 2006). However, in one projection derived
64 from a combination of various models and ice core data, Frieler et al. (2015) state a possible
65 increase in Antarctic accumulation on the continental scale of approximately $5\% \text{ K}^{-1}$. In some
66 parts of Antarctica, higher accumulation would lead to increased ice flow and thus dynamical
67 ice loss, which would reduce the total mass gain (Harig and Simons, 2015; Winkelmann et al.,
68 2012). Thus, for modelling and calculation of the Antarctic mass balance, precipitation
69 amounts and precipitation regimes have to be known as exactly as possible.

70 A second driver for studying Antarctic precipitation is that the ice of Antarctica is an
71 unparalleled climate archive: ice cores up to 800.000 years old yield crucial information about
72 palaeotemperatures and the past constitution of the atmosphere (e.g. EPICA community
73 members, 2004). To derive former air temperatures from ice cores, the stable-isotope ratios of
74 water are used primarily. A linear spatial relationship has been found between mean annual
75 stable isotope ratios in Antarctic precipitation and annual mean air temperature at the
76 deposition site although the isotope ratios depend in a complex way on mass-dependent
77 fractionation processes during moisture transport and precipitation formation (Dansgaard,
78 1964). This spatially derived linear relationship has been found not to hold temporally,
79 however (Jouzel et al., 2003; Jouzel, 2014). Apart from air temperature, several other factors
80 influence the stable isotope ratio, such as seasonality of precipitation, location of and
81 conditions at the moisture sources and conditions along moisture transport paths (e.g.
82 Sodemann and Stohl, 2009; Sodemann et al., 2008, Jouzel et al., 2003; Noone et al., 1999;
83 Schlosser, 1999). Thus, for a correct interpretation of the ice core data a thorough
84 understanding of the atmospheric processes responsible for the precipitation is needed, as it
85 was the precipitation that ultimately formed the glacier ice investigated in the cores. In
86 particular, information about precipitation mechanisms, moisture sources and transport paths,
87 and atmospheric conditions at the final deposition site is required.

88 Measuring Antarctic precipitation is a challenge, not only due to the remoteness and extreme
89 climate of the continent, but also due to difficulties in distinguishing between drifting/blowing
90 snow and falling precipitation. The latter is due to the high wind speeds that typically
91 accompany precipitation events in coastal areas. In the interior of the continent, while wind
92 speeds are lower than at the coast, the threshold for drifting snow is often lower due to lower
93 snow densities as well. Measurements are also complicated by the extremely small amounts
94 of precipitation produced in the cold and dry air. Precipitation measurements with optical

95 devices may hold some hope for improved data in the future, but these instruments are
96 currently in the testing phase in Antarctica (Colwell, pers. comm.). In light of the lack of
97 observations, atmospheric models have become increasingly useful tools to investigate
98 Antarctic precipitation (Bromwich et al., 2004; Schlosser et al., 2010a; 2010b; 2008; Noone
99 and Simmons, 2002; Noone et al., 1999; Noone and Simmons, 1998).

100 This study focusses on the differences in the precipitation regime of two contrasting years
101 within the short measuring period, motivated by the consequences different precipitation/flow
102 regimes have on stable isotope interpretation. The present investigation concentrates on the
103 years 2009 and 2010. These years were chosen because they showed striking contrasting
104 temperature and precipitation anomalies, particularly in the winter seasons. Fogt (2010)
105 reports that temperatures in the Antarctic were persistently above average in the mid-to-lower
106 troposphere during the winter of 2009. The positive surface temperature anomalies were most
107 marked in East Antarctica. In 2010, the picture was very different from 2009, with generally
108 below-average temperatures on the East Antarctic plateau in winter and spring (Fogt, 2011).

109

110

111 **2 Study site**

112 Dome C (75.106 °S, 123.346 °E, elevation 3233m) is one of the major domes on the East
113 Antarctic ice sheet. Its mean annual temperature is -54.5 °C, and the mean annual
114 accumulation derived from ice cores amounts to 25 mm water equivalent (w.e.)/yr. Several
115 deep ice cores have been retrieved at Dome C, the first one in 1977/78, reaching a depth of
116 906 m, corresponding to an age of approximately 32,000 yr. The thermally drilled core was
117 retrieved during the International Antarctic Glaciological Project (Lorius, 1979).

118 The oldest ice to date has been obtained at Dome C through the European deep drilling
119 project EPICA (European Project for Ice Coring in Antarctica). The drilling was completed in
120 January 2006; at the base of the 2774.15 m long ice core the age of the ice was estimated to be
121 800.000 yr, thus covering eight glacial cycles (EPICA community members, 2004). To
122 support the EPICA drilling operation, the French-Italian Antarctic wintering base Dome
123 Concordia became operational in 2005.

124

125

126 3 Previous work

127 Precipitation conditions in the interior of Antarctica are very different from those in coastal
128 areas. Whereas precipitation at the coast is usually caused by frontal systems of passing
129 cyclones that form in the circumpolar trough (e.g. Simmonds et al., 2002), in the interior
130 different precipitation mechanisms are at play. On the majority of days, only diamond dust,
131 also called clear-sky precipitation, is observed. It forms due to radiative cooling in a nearly
132 saturated air mass. Although diamond dust is predominant temporally, it does not necessarily
133 account for the largest fraction of the total yearly precipitation. It has been shown that a few
134 snowfall events per year can bring up to 50% of the total annual precipitation (Braaten et al.,
135 2000; Reijmer and van den Broeke, 2003; Fujita and Abe, 2006; Schlosser et al., 2010a;
136 Gorodetskaya et al., 2013). Those events are due to amplification of Rossby waves in the
137 circumpolar westerlies, which increases the meridional transport of heat and moisture
138 polewards. In extreme cases this can even mean a transport from the Atlantic sector across the
139 continent to the Pacific side (Sinclair, 1981; Schlosser et al., 2015b) The relatively moist and
140 warm air is orographically lifted over the ice sheet, followed by cloud formation and/or
141 precipitation (Noone et al, 1999; Massom et al., 2004; Birnbaum et al., 2006; Schlosser et al.,
142 2010). Except for the study by Fujita and Abe (2006), all of these investigations were based
143 on model and AWS data, rather than daily precipitation measurements.

144 For a long time it was believed in ice core studies that precipitation represented in Antarctic
145 ice cores is formed close to the upper boundary of the temperature inversion layer assuming
146 that the largest moisture amounts are found where the air temperature is highest (Jouzel and
147 Merlivat, 1984). This is a very simplified view that is, however, widely used in ice core
148 studies. It assumes that there are basically no multiple temperature inversions and that
149 humidity is only dependent on temperature through the Clausius-Clapeyron equation, which
150 describes the temperature dependence of vapour pressure. This would mean that humidity and
151 temperature inversions would always have a similar profile. However, more recent studies
152 have shown that humidity inversions are parallel to the temperature inversion only in 50% of
153 the cases, and often multiple humidity (and temperature) inversions occur (Nygard et al.,
154 2013). In particular, the local cycle of sublimation and re-sublimation (deposition) is poorly
155 known, but it is important for both mass balance and isotope fractionation studies.

156 At Dome Fuji, at an elevation of 3810m, the air can be so dry that, in spite of the advection of
157 warm and moist air related to amplified Rossby waves, no precipitation is observed at the site.
158 However, this synoptic situation can cause a strong warming in the lower boundary layer

159 (particularly during blocking situations) due to a combination of warm air advection and
160 removal of the temperature inversion layer by increased wind speed that induces mixing and
161 cloud formation, which in turn increases downwelling longwave radiation (Enomoto et al,
162 1998; Hirasawa et al., 2000). Increased precipitation amounts can also be observed after a
163 snowfall event when the warm air advection has ended, but increased levels of moisture
164 prevail, which can lead to extraordinarily high amounts of diamond dust precipitation
165 (Hirasawa et al., 2013). In West Antarctica, intrusions of warm, marine air can lead to
166 increased cloudiness, precipitation and air temperature. A change in the frequency or intensity
167 of such warm air intrusions could have a large effect on West Antarctic climate if the mean
168 general circulation changed (Nicolas and Bromwich, 2011).

169 Moisture origin has been investigated in various studies using back-trajectory calculations
170 employing different models and methods (Scarcilli et al., 2010; Sodemann and Stohl, 2009;
171 Sodemann et al. 2008; Suzuki et al., 2008; Reijmer et al., 2002). In a recent study by
172 Dittmann et al. (2015), who investigated precipitation and moisture sources at Dome F for
173 precipitation events in 2003, it was estimated that the origin of the moisture was farther south
174 (on average at 50°S) and the transport occurred lower in the atmosphere (approximately at the
175 500-hPa level) than previously assumed in ice core studies.

176 Dome C is a deep ice core drilling site. However, the measurements presented here are the
177 first derived from fresh snow samples at this site. A similar study, if only for a period of
178 approximately one year, was carried out by Fujita and Abe (2006) at Dome Fuji (see Fig. 1),
179 another deep-drilling site in East Antarctica. They investigated daily precipitation data
180 together with measurements of stable isotope ratios of the precipitation samples. Temporal
181 variations of $\delta^{18}\text{O}$ were highly correlated with air temperature. Half of the annual
182 precipitation resulted from only 11 events (18 days), without showing any seasonality. The
183 other half was due to diamond dust. Similar results were found in studies by Schlosser et al.
184 (2010a), at Kohnen Station (see Fig. 1) and by Reijmer and Van den Broeke (2003), who used
185 data from automatic weather stations in Dronning Maud Land. The precipitation-weighted
186 temperature was significantly higher than the mean annual surface temperature because the
187 precipitation events were related to warm-air advection, which leads to a warm bias in the
188 $\delta^{18}\text{O}$ record.

189

190 **4 Data and methods**

191 **4.1 Precipitation**

192 Daily precipitation measurements were initiated at Dome C in 2006, and have, with some
193 interruptions, been continued until today. Daily precipitation amounts are measured using a
194 wooden platform set up at a distance of 800 m from the main station, at a height of 1 m above
195 the snow surface to avoid contributions from low drifting snow. For the same reason, the
196 platform is surrounded by a rail of approximately 8 cm height. The measurements include
197 precipitation sampling and analysis of stable water isotopes ($\delta^{18}\text{O}$, δD) of the samples.
198 Additionally, the crystal structure of the precipitation is analysed in order to distinguish
199 between diamond dust, snowfall, and drift snow. Diamond dust consists of extremely fine ice
200 needles whereas synoptic snowfall shows various types of regular snow crystals, which tend
201 to be broken in case of drifting/blowing snow. The snow crystal type depends on air
202 temperature during formation in the cloud. Samples of mixed crystal types can also occur.

203 While errors of the precipitation measurements cannot be quantified, it is understood that they
204 can exceed 100% given the extremely small precipitation amounts.

205 The Dome C precipitation series is the first and so far only multi-year precipitation/stable
206 isotope series at an Antarctic deep ice core drilling site.

207

208 **4.2 AWS data**

209 The Antarctic Meteorological Research Center (AMRC) and Automatic Weather Station
210 (AWS) Program are sister projects of the University of Wisconsin-Madison funded under the
211 United States Antarctic Program (USAP) that focus on data for Antarctic research support,
212 providing real-time and archived weather observations and satellite measurements and
213 supporting a network of automatic weather stations across Antarctica.

214 The current AWS at Dome C was set up by the AMRC, in December 1995. The station
215 measures the standard meteorological variables of air temperature, pressure, wind speed, wind
216 direction, and humidity. Data can be obtained from <http://amrc.ssec.wisc.edu>. Note that an
217 initial AWS (named Dome C) had been set up in 1985, however, at a distance of about 70 km
218 from the current site. Thus, only data from the new station (Dome C II) are used in the present
219 study.

220

221 **4.3 WRF Model Output from the AMPS Archive**

222 In addition to the observations described above, this study uses numerical weather prediction
223 (NWP) model output for analysis of the synoptic environments of the target years, of
224 precipitation processes, and of events. The output is from forecasts of the Weather Research
225 and Forecasting (WRF) Model (Skamarock et al., 2008) run under the Antarctic Mesoscale
226 Prediction System (AMPS) (Powers et al., 2003; 2012), a real-time NWP capability that
227 supports the weather forecasting for the United States Antarctic Program (USAP). The (U.S.)
228 National Center for Atmospheric Research (NCAR) has run AMPS since 2000 to produce
229 twice-daily forecasts covering Antarctica with model grids of varying resolutions. The AMPS
230 WRF forecasts have been stored in the AMPS Archive and used extensively in studies (e.g.
231 Monaghan et al., 2005; Seefeldt and Cassano, 2008; Schlosser et al., 2008; Seefeldt and
232 Cassano, 2012). For 2009 and 2010, the WRF output over the Dome C region reflects a
233 forecast domain with a horizontal grid spacing of 15 km, employing 44 vertical levels
234 between the surface and 10 hPa. This 15-km grid was nested within a 45-km grid covering
235 the Southern Ocean, and Fig. 2 shows these domains.

236 Model output from AMPS has been verified through various means over the years. Multi-
237 year AMPS forecast evaluations have been conducted (Bromwich et al., 2005), and WRF's
238 ability for the Antarctic in particular has been confirmed (Bromwich et al., 2013). AMPS's
239 and WRF's Antarctic performance has also been documented in a number of case and process
240 studies (e.g. Bromwich et al., 2013; Nigro et al., 2011; 2012; Powers, 2007). For model
241 development within AMPS, verification for both warm and cold season periods is performed
242 prior to changes in model versions or configurations (Powers et al., 2012). The reliability of
243 AMPS WRF forecasts is also reflected in their demand from international Antarctic
244 operations and field campaign forecasting efforts (see e.g. Powers et al., 2012). Lastly,
245 similarly to how it is used here, AMPS output has been a key tool in previous published
246 studies of Antarctic precipitation related to ice core analyses (Schlosser et al., 2008; 2010a;
247 2010b).

248 In this study the WRF output from the AMPS archive is used to study both the synoptic
249 patterns/general atmospheric circulation and the local conditions related to the precipitation
250 regimes and events in the years compared. The WRF forecasts provide reliable depictions of
251 conditions and their evolution.

252

253 **5 Results**

254 **5.1 Temperature and precipitation**

255 Figure 3a shows the mean monthly air temperature observed at the Dome C AWS for 2009
256 and 2010 as well as the mean of 1996-2014. The mean annual cycle exhibits the typical
257 coreless winter (van Loon, 1967) with a distinct temperature maximum in summer
258 (December/January), which has no counterpart in winter, where the months May to August
259 show relatively similar values. This is due to a combination of the local surface radiation
260 balance and warm air intrusions. During the first part of the polar night, with the lack of short-
261 wave radiation, an equilibrium of downwelling and upwelling longwave radiation is reached;
262 advection of relatively warm air from lower latitudes further reduces the possibility for
263 cooling. Thus the temperature does not decrease significantly after May (King and Turner,
264 1997; Schwerdtfeger 1984).

265 While during the summer months little difference is seen between 2009 and 2010 the winter
266 months are strikingly different. The lowest mean July temperature of the station record occurs
267 in 2010 with a value of $-69.7\text{ }^{\circ}\text{C}$. This is the lowest monthly mean ever observed at Dome C,
268 $5.9\text{ }^{\circ}\text{C}$ lower than the average 1996-2014, corresponding to a deviation of 1.7σ , σ being the
269 standard deviation. In contrast, the highest July mean temperature is found in 2009; with a
270 value of $-54.9\text{ }^{\circ}\text{C}$, it was $8.9\text{ }^{\circ}\text{C}$ higher (corresponding to 2.5σ) than the long-term July mean
271 and the only July mean that exceeded $-60\text{ }^{\circ}\text{C}$. In Figure 3b, observed daily mean temperatures
272 and daily precipitation sums for the years 2009 and 2010 are displayed. Again, the differences
273 between the two years are most striking in winter. In 2009, the temperature variability is very
274 high, and several warming events with temperatures up to almost $-30\text{ }^{\circ}\text{C}$ can be seen.
275 Minimum temperatures are rarely lower than $-70\text{ }^{\circ}\text{C}$ whereas in 2010, minima are close to -80
276 $^{\circ}\text{C}$. The highest temperature in the winter of 2010 was only slightly above $-50\text{ }^{\circ}\text{C}$. The winter
277 2009 thus was not only a “coreless winter”, but had a “warm” core due to the high number of
278 warm air intrusions.

279 A very high precipitation value of 1.36 mm on 9 February 2010, followed by 0.67 mm on 10
280 February, both classified as diamond dust from the photographic crystal analysis, stems from
281 only one event around 9 February.. Considering the extremely low density of diamond dust, a
282 diamond dust amount of more than 1mm/day at first, seemed to be unlikely. However, the
283 model data do show a precipitation event connected to warm air advection from the north (see
284 below) for this day, which would indicate the occurrence of snowfall rather than diamond

285 dust. Most likely a mixture of crystal types was found during this event with the diamond dust
286 on top of the snow crystals, which possibly led to the classification of the event as diamond
287 dust. (Note that the crystal classification was carried out purely from photographs by an
288 expert at the Avalanche Institute in Italy and that snow crystals are also comparatively small at
289 the temperatures prevailing at Dome C). Also, it was found that increased amounts of
290 diamond dust can prevail after snowfall events when humidity is still increased compared to
291 the average, but not large enough to cause real snowfall. The precipitation totals for May to
292 September are 12.0 mm w.e. for 2009 and 4.3 mm w.e. for 2010. Daily sums exceed 0.25 mm
293 only three times in 2010, but 16 times in 2009. Usually, high daily precipitation amounts are
294 associated with relative maxima in air temperature. In general, the winter of 2010 was cold
295 and dry, whereas 2009 was relatively warm and moist compared to the long-term average.

296 Figure 4a shows monthly precipitation amounts for 2009 and 2010, distinguishing between
297 diamond dust, hoar frost, and snowfall; Figure 4b gives the relative frequencies of the three
298 different observed types of precipitation for both years. Again, large differences between 2009
299 and 2010 are found. While approximately half of the precipitation fell as snow in 2009, less
300 than a quarter of the total precipitation stemmed from snowfall in 2010, when mostly diamond
301 dust was observed. As seen before, the winter months of May to September exhibit the
302 largest differences. In particular, the extremely “warm” July of 2009 brought high amounts of
303 snowfall. The lowest amounts of precipitation are seen in austral summer 2009/2010, with no
304 precipitation observed in November and only very small amounts in December and January.

305 The total amount of precipitation measured on the raised platform is 16.5 mm w.e. for 2009
306 and 13.4 mm w.e. for 2010, compared to the mean annual accumulation of 25 mm w.e.
307 derived from firn core and stake measurements (Frezzotti et al., 2005). From the available
308 data it cannot be determined whether the difference is due to snow removed from the
309 measuring platform by wind or sublimation or snow added to the snow surface at the stake
310 array by wind (blowing or drifting snow) or deposition (re-sublimation).

311

312 **5.2 Atmospheric flow conditions**

313 **5.2.1 Synoptic analyses with AMPS archive data**

314 The synoptic situations that caused precipitation at Dome C were analysed using WRF output
315 data from the AMPS archive. In particular, fields of 500hpa geopotential height and 24-h

316 precipitation were used. For the 500hPa geopotential height information the 12-h forecast was
317 utilized. For 24-h precipitation, the 12-36h forecast sums of precipitation (rather than 0-24h)
318 were used to allow for model spin up of clouds and microphysical fields. This is considered
319 long enough for moist process spin-up, but avoids error growth reflected in longer forecast
320 times (Bromwich et al., 2005).

321 For all precipitation events with observed daily sums exceeding 0.2mm, the synoptic
322 situations that caused the precipitation were investigated. In total, 29 events were studied, 20
323 in 2009 and 9 in 2010. For 2009 (2010), the model showed precipitation at Dome C in 44%
324 (50%) of the studied cases and precipitation in the vicinity in 33 (25) % of the cases; no
325 precipitation was shown in the model in 22 (25) % of the cases. In total, approximately half of
326 the precipitation events were represented well by the model, one quarter showed synoptic
327 events that did not bring precipitation exactly at the location and time of the measurements,
328 and one quarter of the cases were not forecast by the model at all. An exact quantitative
329 analysis of the model skill using the entire data series starting in 2006 is ongoing and the
330 results will be more meaningful than those of only two, not very typical, years.

331 Generally, snowfall events were found to be associated with an amplification of the Rossby
332 waves in the circumpolar westerlies, which causes a northerly flow across the Dome C region
333 between a trough to the west and an upper-level ridge to the east of Dome C. This northerly
334 flow brings relatively warm and moist air from as far as 35 °S - 40 °S to the East Antarctic
335 plateau, leading to orographic precipitation when it is forced to ascend on the way from the
336 coast to the high-altitude interior. Variations of this general situation are due to the duration of
337 the flow pattern (e.g. whether there is a blocking anticyclone or not) and the strength of the
338 upper-level ridge, which determines how far north the main moisture origin is situated. Figure
339 5 shows an example of this synoptic situation typical for snowfall events. In the 500hPa
340 geopotential height field (Fig. 5a) for 13 September 2009 the amplified ridge that leads to a
341 northerly flow towards Dome C can be seen slightly east of Dome C, with an axis tilted in a
342 NE-SW direction. Figure 5b displays the 24-h precipitation caused by the N-NE flow onto the
343 continent. Dome C is situated at the southeastern edge of the precipitation area.

344 A frequent occurrence of the synoptic situation described (as it was the case in 2009) means a
345 more northern mean moisture source than on average, which has to be taken into account for
346 deriving air temperature from stable isotopes. (A detailed study using trajectory calculations
347 for all observed precipitation events at Dome C is ongoing.) It was also found to be typical for
348 precipitation events at Dome C that the main westerly flow is split into a northern branch that

349 remains zonal, whereas the southern branch starts meandering with a strong meridional
350 component. This is observed more often at Dome C than at Dome F (Dittmann et al., 2015) or
351 at Kohlen Station (Schlosser et al., 2010a).

352 Figure 6 presents an example for a case with no precipitation in the model, but relatively large
353 observed precipitation amounts. The 500hPa geopotential height field (Fig. 6a) shows a
354 cutoff-high west of Dome C on the day after the precipitation event shown in Figure 5. The
355 remaining atmospheric moisture is not sufficient to produce precipitation in the model (Fig.
356 6b), but it does lead to remarkably high amounts of diamond dust and/or hoar frost (0.7 mm
357 observed during this event). This synoptic situation was also found by Hirasawa et al. (2013)
358 in a detailed study of the synoptic conditions and precipitation during and after a blocking
359 event at Dome Fuji. (Note that neither diamond dust nor hoar frost formation is specifically
360 parameterized in the model.) In 2010, the flow was mainly zonal and the synoptic situations
361 described above were much less frequent than in 2009 and not as strongly developed.

362 Using the WRF output, monthly composite fields of 500hPa-geopotential height were
363 calculated to compare the general flow conditions in 2009 and 2010. Figure 7 shows the
364 composite mean 500-hPa geopotential height for July 2009 and 2010, respectively. Even in
365 the monthly mean, the distinct upper-level ridge in 2009 that projects onto the East Antarctic
366 plateau and leads to warm air advection and increased precipitation at Dome C is clearly seen.

367 In 2010, in the monthly average, the flow was mainly zonal, which reduced the meridional
368 exchange of heat and moisture, thus leading to lower temperatures and less precipitation in the
369 interior of the Antarctic continent.

370

371 **5.2.2 Southern Annular Mode**

372 The occurrence of high-precipitation events on the Antarctic plateau due to amplification of
373 Rossby waves is often connected to a strongly positive phase of the Southern Annular Mode
374 (SAM). The SAM is the dominant mode of atmospheric variability in the extratropical
375 Southern Hemisphere. It is revealed as the leading empirical orthogonal function in many
376 atmospheric fields (e.g. Thompson and Wallace, 2000), such as surface pressure, geopotential
377 height, surface temperature, and zonal wind (Marshall, 2003). Since pressure fields from
378 global reanalyses commonly used to study the SAM are known to have relatively large errors
379 in the polar regions, Marshall (2003) defined a SAM index based on surface observations. He

380 calculated the pressure differences between 40 °S and 65 °S using data from six mid-latitude
381 stations and six Antarctic coastal stations to calculate the corresponding zonal means. A large
382 (small) meridional pressure gradient corresponds to a positive (negative) SAM index. The
383 positive index means strong, mostly zonal westerlies and comparatively little exchange of
384 moisture and energy between middle and high latitudes, which leads to a general cooling of
385 Antarctica, except for the Antarctic Peninsula that projects into the westerlies. A negative
386 SAM index is associated with weaker westerlies and a larger meridional flow component.

387 Figure 8 shows the monthly mean SAM index for 2009 and 2010 (data can be found at
388 <http://www.nerc-bas.ac.uk/icd/gjma/sam.html>). Whereas in the winter months (May to
389 September) of 2009 the SAM index was generally negative (with the exception of a weakly
390 positive value in June), 2010 has positive indices from April to August, with strongly positive
391 values in June and July, and only a weakly negative index in September. This is consistent
392 with the pattern of a strong zonal flow with few precipitation events at Dome C due to
393 amplified ridges in the winter of 2010, with the opposite situation holding in 2009. The
394 highest SAM index is found in November 2010; however, in austral summer the relationship
395 between the SAM index and precipitation seems to be less straightforward. The differences
396 between 2009 and 2010 are not extraordinarily high compared to other years (e.g. 2001/2002
397 as seen at <http://www.nerc-bas.ac.uk/public/icd/gjma/newsam.spr.pdf>), however, qualitatively
398 they are in agreement with the observed flow pattern. Furthermore, it should be kept in mind
399 that SAM explains only about one third of the atmospheric variability in the Southern
400 Hemisphere (Marshall, 2007) and that the SAM index alone gives no information about the
401 location of respective ridges and troughs in a highly meridional flow pattern.

402

403 **5.2.3 Zonal wave number 3**

404 Another method to investigate the general atmospheric flow conditions is to analyse spatial
405 and temporal variations of the quasi-stationary zonal waves in the Southern Hemisphere. In
406 this study zonal wave number 3 (ZW3) is used. While the atmospheric circulation in the
407 Southern Hemisphere appears strongly zonal (or symmetric), there is a significant non-zonal
408 (asymmetric) component and ZW3 represents a significant proportion of this asymmetry. It is
409 a dominant feature of the circulation on a number of different time scales (e.g. Karoly, 1989),
410 is responsible for 8% of the spatial variance in the field (van Loon and Jenne, 1972), and
411 contributes significantly to monthly and interannual circulation variability (e.g. Trenberth,

412 1990; Trenberth and Mo, 1985). The asymmetry is revealed when the zonal mean is
413 subtracted from the geopotential height field thereby creating a coherent pattern of zonal
414 anomalies, with the flow associated with these patterns becoming apparent. ZW3 has
415 preferred regions of meridional flow, which influence the meridional transport of heat and
416 moisture into and out of the Antarctic. Raphael (2004) defined an index of ZW3 based on its
417 amplitude (effectively the size of the zonal anomaly) at 50°S showing that ZW3 has
418 identifiable positive and negative phases associated with the meridionality of the flow. A
419 positive value for this index indicates more meridional flow (large zonal anomaly) and a
420 negative value more zonal flow (small zonal anomaly). Note that the ZW3 index used here
421 does not fully capture the shift in phase of the wave. However, Raphael (2004) found that the
422 net effect is a small reduction in the amplitude of the wave, but the sign of the index is not
423 influenced. A new approach for identifying Southern Hemisphere quasi-stationary planetary
424 wave activity that allows variations of both wave phase and amplitude is described in a recent
425 study by Irving and Simmonds (2015).

426 Figure 9a shows the monthly mean ZW3 index for the period 2009–2010. From June to
427 September 2009 the ZW3 index was largely positive except for a comparatively small
428 negative excursion in July. On the contrary, from June to September 2010 it was negative. The
429 asymmetry in the circulation suggested by the index is shown in Figure 9b (July 2009) and 9c
430 (July 2010). These figures were created by subtracting the long-term zonal mean at each
431 latitude, from the mean 500-hPa geopotential height field in July 2009 and 2010, respectively.
432 The flow onto Dome C suggested by the alternating negative and positive anomalies is
433 northerly in July 2009, but has a strong zonal component in July 2010. This information given
434 by the ZW3 index and the patterns of zonal anomalies is consistent with that suggested by the
435 SAM.

436

437 **6 Discussion and Conclusion**

438 In the present study that was motivated by stable water isotope studies, atmospheric
439 conditions of the two contrasting years 2009 and 2010 at the Antarctic deep-drilling site
440 Dome C, on the East Antarctic Plateau were investigated using observational precipitation and
441 temperature data and data from a mesoscale atmospheric model. The observations from Dome
442 C represent the first and only multi-year series of daily precipitation/stable isotope
443 measurements at a deep-drilling site, even though “multi” means only nine years in this case.

444 The differences between the two years 2009 and 2010 were most striking in winter. Whereas
445 2009 was relatively warm and moist due to frequent warm air intrusions connected to
446 amplification of Rossby waves in the circumpolar westerlies, the winter of 2010 was
447 extremely cold and dry, with the lowest monthly mean July temperature observed since the
448 beginning of the AWS measurements in 1996. This can be explained by the prevailing strong
449 zonal flow in the winter of 2010, related to a strongly positive SAM index and a negative
450 ZW3 index. Also, the frequency distribution of the various precipitation types was largely
451 different in 2009 and 2010, with snowfall prevailing in 2009 whereas diamond dust was
452 dominant in 2010.

453 Similarly striking differences in weather conditions of 2009 and 2010 were seen in other parts
454 of East Antarctica. Gorodetskaya et al. (2013) found that accumulation in 2009 was eight
455 times higher than in 2010 at the Belgian year-round station “Princess Elisabeth”. At this
456 location, the temperature was also higher in 2009 than in 2010, particularly in fall/early
457 winter. The findings are supported by Boening et al. (2012), who used observations from
458 GRACE (Gravity Recovery And Climate Experiment) and found an abrupt mass increase on
459 the East Antarctic ice sheet in the period 2009-2011. Similarly, Lenaerts et al. (2013)
460 investigated snowfall anomalies in Dronning Maud Land, East Antarctica. They state that the
461 large positive anomalies of accumulation found in 2009 and 2011 stand out in the past
462 approximately 60 years although comparable anomalies are found further back in time.

463 Distinguishing between the different forms of precipitation, namely diamond dust, hoar frost
464 and dynamically caused snowfall, is important for both mass balance and ice core
465 interpretation. For mass balance, the different precipitation types do not have to be known if
466 the surface mass balance is determined as an annual value from snow pits, firn/ice cores or
467 stake arrays. For temporally higher resolved precipitation measurements, however, a fraction
468 of both hoar frost and diamond dust might be just a part of the local cycle of sublimation and
469 deposition (re-sublimation), thus representing no total mass gain. More detailed
470 measurements are thus necessary to allow a better understanding of the processes involved.
471 This also applies to isotopic fractionation during this cycle; continuous measurements of
472 water vapour stable isotope ratios (e.g. Steen-Larsen et al., 2013) should be included here.

473 For ice core interpretation, the problem generally becomes more complex. Diamond dust is
474 observed during the entire year without a distinct seasonality. Therefore a signal from an ice
475 core property measured in the ice (in contrast to measured in the air bubbles) will have
476 contributions from diamond dust that stem nearly equally from all seasons. Although snowfall

477 events are not very frequent at deep ice core drilling sites, they can account for a large
478 percentage of the total annual precipitation/accumulation at those locations. If these events
479 have a seasonality that has changed between glacial and interglacials, a large bias will be
480 found in the temperature derived from the stable isotopes in ice cores. Today, the frequency of
481 such snowfall events shows a high inter-annual variability, but both frequency and seasonality
482 of the events might be different in a different climate due to changes in the general
483 atmospheric circulation and in sea ice extent (e.g. Godfred-Spenning and Simmonds, 1996).
484 Since it was found that snowfall events are connected to the synoptic activity in the
485 circumpolar trough, it is plausible that the seasonality of such events was different during
486 glacial times because the sea ice edge and the mean position of the westerlies were
487 considerably farther north than today. This influences the zone of the largest meridional
488 temperature gradient, thus the largest baroclinicity and consequently cyclogenesis. A larger
489 sea ice extent might reduce the number of snowfall events in the Antarctic interior in winter
490 by pushing the zone of largest baroclinicity northwards. However, it is not possible to assess
491 such hypotheses using observational data since the instrumental period, with few exceptions,
492 started in Antarctica not before the IGY (International Geophysical Year) 1957/58. However,
493 modelling studies can be supported by studies of the physical processes in the atmosphere
494 using recent data, and, in particular, cases of extreme situations can be helpful here. Even if
495 the full amplitude of the change between glacial and interglacial climates is not observed,
496 extrema can give insight into the sign and kind of the reaction of the system to a change in
497 one or several atmospheric variables.

498 Another implication for ice core interpretation derived from the present study is that a more
499 northern moisture source does not necessarily mean larger isotopic fractionation (which is
500 usually assumed in ice core studies (e.g. Stenni et al., 2001; 2010). Even without a
501 quantitative determination of the moisture source it can be said that in an increased meridional
502 flow, as in 2009, heat and moisture transport from relatively low latitudes is increased, too,
503 and leads to higher precipitation stemming from more northern oceanic sources than on
504 average. Although the temperature at the main moisture source is higher than on average for a
505 more northern moisture source, the depletion in heavy isotopes is comparatively small
506 because the temperature at the deposition site is also clearly higher than on average due to the
507 warm air advection, which reduces the temperature difference between the moisture source
508 region and the deposition site, thus the amount of isotopic fractionation.

509 Looking towards future work, the results here indicate that a combination of process studies
510 using recent data and modelling of the atmospheric flow conditions on larger time scales will
511 lead to a better quantitative interpretation of ice core data. Apart from the factors influencing
512 precipitation itself, it has become clear recently that post-depositional processes between
513 snowfall events are more important than previously thought because, additionally to processes
514 within the snowpack, the interaction between the uppermost parts of the snowpack and the
515 atmosphere is very intense (Steen-Larsen et al., 2013). Parallel measurements of stable
516 isotope ratios of water vapour and surface snow, combined with meteorological data will give
517 more insight into these processes in Antarctica.

518 Altogether, this means that, compared to years with predominantly zonal flow (which is the
519 more frequent situation), in years with enhanced meridional flow (negative SAM index,
520 positive ZW3 index) higher temperatures and higher amounts of precipitation that is less
521 depleted of heavy isotopes are expected at Dome C and comparable interior sites in
522 Antarctica. This is particularly valid for the colder seasons.

523 The relationship between air temperature and stable isotopes of Antarctic precipitation/ice is
524 anything else but straightforward, since the isotope ratio measured in an ice core (or in the
525 snow) is the result of a complex precipitation history that is strongly influenced by the
526 synoptics and general atmospheric flow conditions, followed by post-depositional processes.
527 Without thorough knowledge of all the processes involved a quantitatively correct derivation
528 of paleo temperatures from ice core stable water isotopes is thus not possible.

529

530 **Author contribution**

531 BS is responsible for the precipitation measurements, MV and AC for the crystal analysis.
532 MR did the ZW3 study. MD and KW assisted with software development. ES prepared the
533 manuscript with contributions from JP, KW, MR, and BS.

534

535

536 **Acknowledgements**

537 The precipitation measurements at Dome C have been conducted in the framework of the
538 Concordia station glaciology and ESF PolarCLIMATE HOLOCLIP projects funded in Italy

539 by PNRA-MIUR. This is a HOLOCIP publication number xx. The present study is financed
540 by the Austrian Science Funds (FWF) under grant P24223. AMPS is supported by the U.S.
541 National Science Foundation, Division of Polar Programs. We appreciate the support of the
542 University of Wisconsin-Madison Automatic Weather Station Program with the Dome C II
543 data set. (NSF grant numbers ANT-0944018 and ANT-12456663). We thank Gareth Marshall
544 for providing the SAM indices online. We thank all winterers at Dome C, who did the
545 precipitation sampling. We also thank our editor, Heini Wernli, and Harald Sodemann and
546 two anonymous reviewers for helpful comments that improved the manuscript.

547

548

549

550

551

552

553

554

555

556

557

558

559

560

561

562

563

564

565

566 **References**

567

568 Birnbaum, G., Brauner, R., and Ries, H.: Synoptic situations causing high precipitation rates
569 on the Antarctic plateau: observations from Kohnen Station, Dronning Maud Land , Antarctic
570 Science, 18 (2), pp. 279-288, doi: 10.1017/S0954102006000320, 2006.

571 Boening, C., Lebsock, M., Landerer, F., and Stephens, G. : Snowfall-driven mass change on
572 the East Antarctic ice sheet. Geophys. Res. Let., 39, L21501, doi:10.1029/GL053316, 2012.

573 Braaten, D. A.: Direct measurements of episodic snow accumulation on the Antarctic polar
574 plateau. J. Geophysic. Res., 105, (D9) 10,119-10,128, 2000.

575 Bromwich, D. H: Snowfall in high southern latitudes. Rev. Geophys., 26(1) 149-168, 1988.

576 Bromwich, D. H., Guo, Z., Bai, L., and Chen, Q. : Modeled Antarctic Precipitation. Part I:
577 Spatial and Temporal Variability, *J. Climate*, **17**, 427–447, 2004.

578 Bromwich, D. H., Monaghan, A. J., Manning, K. W., and Powers, J. G.: Real-time forecasting
579 for the Antarctic: An evaluation of the Antarctic Mesoscale Prediction System (AMPS), Mon.
580 Weather Rev., 133, 579-603, 2005.

581 Bromwich, D. H., Otieno, F. O., Hines, K. M., Manning, K. W., and Shilo, E.: Comprehensive
582 evaluation of polar weather research and forecasting performance in the Antarctic. J.
583 Geophys. Res., 118, 274–292, doi: 10.1029/2012JD018139, 2013.

584 Church, J.A., et al.: Sea Level Change. In: Climate Change 2013: The Physical Science Basis.
585 Contribution of Working Group I to the Fifth Assessment Report of the Intergovernmental
586 Panel on Climate Change (Stocker, T.F., D. Qin, D., G.K. Plattner, G. K., M. Tignor, M.,
587 Allen, S. K., Boschung, J., Nauels, A., Xia, Y., Bex, V., and Midgley, P. M. (eds.)),
588 Cambridge University Press, Cambridge, United Kingdom and New York, NY, USA, 2013.

589 Dansgaard, W.: Stable isotopes in precipitation, *Tellus*, XVI (4), 436-468, 1964.

590 Dittmann, A., Schlosser, E., Masson-Delmotte, V., Powers, J. G., Manning, K. W., Werner,
591 M., and Fujita, K.: Precipitation regime and stable isotopes at Dome Fuji, East Antarctica,
592 Atmos. Chem. Phys. Discuss., doi:10.5194/acp-2015-1012, in review, 2016. Enomoto et al.,
593 Winter warming over Dome Fuji, East Antarctica and semiannual oscillation in the
594 atmospheric circulation. J. Geophysic. Res., 103 (D18), 23,103-23,111, 1998.

595 EPICA community members: 8 Glacial cycles from an Antarctic ice core, *Nature*, 429, 623-
596 628, doi:10.1038/nature02599, 2004.

597 Fogt, R. L. In: Arndt, D. S., Baringer, M. O., and M. R. Johnson, Eds., *State of the Climate in*
598 *2009*, 6. Antarctica. Special supplement to *Bull. Am. Meteorol. Soc.*, 91 (7) 125-134, 2010.

599 Fogt, R. L. In: Blunden, J., Arndt, D. S., Baringer, M. O., Eds., *State of the Climate in 2010*,
600 6. Antarctica. Special supplement to *Bull. Am. Meteorol. Soc.*, 92 (6) 161-172, 2011.

601 Frezzotti, M., Pourchet, M., Onelio, F., Gandolfi, S., Gay, M., Urbini, S., Vincent, C., Becagli,
602 S., Gragnani, R., Proposito, M., Severi, M., Traversi, R., Udisti, R., and Fily, M.: Spatial and
603 temporal variability of snow accumulation in East Antarctica from traverse data, *J. Glaciol.*,
604 51(178), 113-123, 2005.

605 Frieler, K., Clark, P. U., He, F., Buizert, C., Reese, R., Ligtenberg, S.R. M., Van den Broeke,
606 M. R., Winkelmann, R., and Levermann, A.: Consistent evidence of increasing Antarctic
607 accumulation with warming, *Nature Climate Change*, 5, 348-352,
608 doi:10.1038/NCLIMATE2574, 2015.

609 Fujita, K., and Abe, O.: Stable isotopes in daily precipitation at Dome Fuji, East Antarctica,
610 *Geophys. Res. Lett.*, 33, L18503, doi:10.1029/2006GL026936, 2006.

611 Godfred-Spenning, C. and Simmonds, I.: An analysis of Antarctic Sea-Ice and Extratropical
612 cyclone associations. *Int. J. Climat.*, 16, 1315-1332, 1996.

613 Gorodetskaya, I.V., N.P.M. Van Lipzig, M. R. Van den Broeke, A. Mangold, W. Boot, and C.
614 H. Reijmer: Meteorological regimes and accumulation patterns at Utsteinen, Dronning Maud
615 Land, East Antarctica: Analysis of two contrasting years. *J. Geophys. Res.*, 118, 1-16,
616 doi:10.1002/jgrd.50177, 2013.

617 Harig, C., and Simons, F. J.: Accelerated West Antarctic ice mass loss continues to outpace
618 East Antarctic gains. *Earth Planet. Sci. Lett.* 415, 134-141, doi:10.1016/j.epsl.2015.01.029,
619 2015.

620 Hirasawa, N., Nakamura, H., and Yamanouchi, T.: Abrupt changes in meteorological
621 conditions observed at an inland Antarctic station in association with wintertime blocking.
622 *Geophys. Res. Lett.*, 27(13), 1911-1914, 2000.

623 Hirasawa, N., Nakamura, H., Motoyama, H., Hayashi, M., and Yamanouchi, T.: The role of
624 synoptic-scale features and advection in a prolonged warming and generation of different

625 forms of precipitation at dome Fuji station, Antarctica, following a prominent blocking event,
626 J. Geophys. Res., 118, 6916-6928, doi:10.1002/jgrd.50532, 2013.

627 Jouzel, J., Vimeux, F., Caillon, N., Delaygue, G., Hoffmann, G., Masson-Delmotte, V., and
628 Parrenin, F.: Magnitude of isotope/temperature scaling for interpretation of central Antarctic
629 ice cores, J. Geophysic. Res., 108 (D12), 4361, doi:10.1029/2002JD002677, 2003.

630 Jouzel, J., in: Heinrich Holland and Karl Turekian (Ed.) Treatise on Geochemistry (Second
631 Edition) 5.8, Elsevier, 213-256, 2014.

632 Karoly, D. J.: Southern Hemisphere circulation features associated with El Nino-Southern
633 Oscillation events, J. Clim., 2, 1239-1251, 1989.

634 King, J. and Turner, J.: Antarctic Meteorology and Climatology. Cambridge Atmospheric and
635 Space Sciences Series, Cambridge University Press, Cambridge, 409pp, 1997.

636 Lenaerts, J. T. M., van Meijgaard, E., Van den Broeke, M.R., Ligtenberg, S. R. M., Horwarth,
637 M., and Isaksson, E.: Recent snowfall anomalies in Dronning Maud Land, East Antarctica, in
638 a historical and future climate perspective. Geophys. Res. Let., 40, 2684-2688,
639 doi:10.1002/grl.50559, 2013.

640 Lorius, C., Merlivat, L., Jouzel, J., and Pourchet, M.: A 30,000 years isotope climatic record
641 from Antarctic ice, Nature, 280, (5724), 644-647, 1979.

642 Marshall, G. J.: Trends in the Southern Annular Mode from observations and reanalyses, J.
643 Clim., 16, 4134-4143, 2003.

644 Marshall, G. J., : Half-century seasonal relationship between the Southern Annular Mode and
645 Antarctic temperatures, Int. J. Climatol., 27, 373-383, 2007.

646 Massom, R., Pook, M. J., Comiso, J. C., Adams, N., Turner, J., Lachlan-Cope, T., and Gibson,
647 T.: Precipitation over the interior East Antarctic ice sheet related to midlatitude blocking-high
648 activity. J. Climate, 17, 1914-1928, 2004.

649 Monaghan, A. J., Bromwich, D. H., Powers, J. G., Manning, K. W.: The Climate of
650 McMurdo, Antarctica, Region as Represented by One Year of Forecasts from the Antarctic
651 Mesoscale Prediction System, J. Climate, 18, 1174-1189, 2005.

652 Monaghan, A. J., Bromwich, D. H., Fogt, R. L., Wang, S., Mayewski, P. A., Dixon, D. A.,
653 Ekaykin, A., Frezzotti, M., Goodwin, I., Isaksson, E., Kaspari, S. D., Morgan, V. I., Oeter, H.,
654 Van Ommen, T. D., Van der Veen, C. J., and Wen, J.: Insignificant change in Antarctic
655 snowfall since the International Geophysical Year. *Science*, 313, 827-831, doi:
656 10.1126/science.1128243, 2006.

657 Nicolas, J. P. and Bromwich, D. H.: Climate of West Antarctica and Influence of Marine Air
658 Intrusions. *J. Climate*, 24, 49-67. doi:10.1175/2010JCLI3522.1, 2011.

659 Nigro, M. A., Cassano, J. J., and Seefeldt, M. W.: A weather pattern-based approach to
660 evaluate the Antarctic Mesoscale Prediction System (AMPS) forecasts: Comparison to
661 automatic weather station observations. *Wea. Forecasting*, 26, 184-198,
662 doi:10.1175/2010WAF2222444.1, 2011.

663 Nigro, M. A., Cassano, J. J., and Knuth, S. L.: Evaluation of Antarctic Mesoscale Prediction
664 System (AMPS) cyclone forecasts using infrared satellite imagery. *Antarctic Science*, 24, 183-
665 192, doi:10.1017/S0954102011000745, 2012.

666 Noone, D., and Simmonds, I.: Implications for the interpretation of ice-core isotope data from
667 analysis of modelled Antarctic precipitation. *Ann. Glaciol.*, 27, 398-402, 1998.

668 Noone, D., and Simmonds, I.: Associations between $\delta^{18}\text{O}$ Of water and climate parameters in
669 a simulation of atmospheric circulation for 1979-95. *J. Clim.*, 15, 3150-3169, 2002.

670 Noone, D., Turner, J., and Mulvaney, R.: Atmospheric signals and characteristics of
671 accumulation in Dronning Maud Land, Antarctica. *J. Geophysic. Res.*, 104 (D16), 19,191-
672 19,211, 1999.

673 Nygard, T., Valkonen, T., and Vihma, T.: Antarctic Low-Tropopause Humidity Inversions: 10-
674 yr Climatology, *J. Climate*, 26, 5205-5219, doi: 10.1175/JCLI-D-12-00446.1, 2013.

675 Powers, J. G., Monaghan, A. J, Cayette, A. M., Bromwich, D. H., Kuo, Y., and Manning, K.
676 W.: Real-time mesoscale modeling over Antarctica. The Antarctic Mesoscale Prediction
677 System. *Bull. Am. Meteorol. Soc.*, 84, 1522-1545, 2003.

678 Powers, J. G.: Numerical prediction of an Antarctic severe wind event with the Weather
679 Research and Forecasting (WRF) Model. *Mon. Wea. Rev.*, 135, 3134-3157, 2007.

680 Powers, J. G., Manning, K. W., Bromwich, D. H., Cassano, J. J., and Cayette, A. M.: A decade
681 of Antarctic science support through AMPS. *Bull. Amer. Meteor. Soc.*, 93, 1699-1712, 2012.

682 Raphael, M. N.: A zonal wave 3 index for the Southern Hemisphere, *Geophys. Res. Lett.*,
683 31(23), doi:10.1029/2004GL020365, 2004.

684 Reijmer C. H, Van den Broeke, M. R., and Scheele, M. P.: Air parcel trajectories and snowfall
685 related to five deep drilling locations in Antarctica based on the ERA-15 dataset, *J. Climate*,
686 15:1957–1968, 2002.

687 Reijmer, C. H. and van den Broeke, M. R.: Temporal and spatial variability of the surface
688 mass balance in Dronning Maud Land, Antarctica. *J. Glaciol.*, 49(167), 512-520, 2003.

689 Ritter, F., Steen-Larsen, H. C., Kipfstuhl, J., Orsi, A., Behrens, M., and Masson-Delmotte, V.:
690 First continuous measurements of water vapor isotopes on the Antarctic Plateau, *Geophys.*
691 *Res. Abstr.*, 16, EGU2014-9721, 2014.

692 Scarchilli, C., Frezzotti, M., and Ruti, P. M.: Snow precipitation at four ice core sites in East
693 Antarctica - provenance, seasonality and blocking factors. *Clim. Dyn.*, 37, 2107-2125,
694 doi:10.1007/s00382-010-0946-4, 2010.

695 Schlosser, E.: Effects of seasonal variability of accumulation on yearly mean $\delta^{18}\text{O}$ values in
696 Antarctic snow, *J. Glaciol.* , 45 (151), 463-468, 1999.

697 Schlosser, E., Duda, M. G., Powers, J. G, Manning, K. W.: The precipitation regime of
698 Dronning Maud Land, Antarctica, derived from AMPS (Antarctic Mesoscale Prediction
699 System) Archive Data. *J. Geophys. Res.*, 113. D24108, doi: 10.1029/2008JD009968, 2008.

700 Schlosser, E., K. W. Manning, K. W., Powers, J. G., Duda, M. G., Birnbaum, G., and Fujita,
701 K.: Characteristics of high-precipitation events in Dronning Maud Land, Antarctica. *J.*
702 *Geophys. Res.*, 115, D14107, doi:10.1029/2009JD013410, 2010.

703 Schlosser, E., Powers, J. G., Duda, M. G., Manning, K. W., Reijmer, C.H., Van den Broeke,
704 M.: An extreme precipitation event in Dronning Maud Land, Antarctica - a case study using
705 AMPS (Antarctic Mesoscale Prediction System) archive data. *Polar Research*,
706 doi:10.1111/j.1751-8369.2010.00164.x, 2010.

707 Schlosser, E., Manning, K. W., Powers, J. G., Gillmeier, S., and Duda, M. G., An extreme
708 precipitation/warming event in Antarctica – a study with Polar WRF, in preparation, 2016.

709 Sodemann, H., and A Stohl. 2009. Asymmetries in the moisture origin of Antarctic
710 precipitation. *Geophys.Res. Letters* 36: L22803. doi:10.1029/2009GL040242.
711

712 Sodemann, H., Masson-Delmotte, V., Schwierz, C., Vinther, B. M. and Wernli, H.,: Inter-
713 annual variability of Greenland winter precipitation sources. Part II: Effects of North Atlantic
714 Oscillation variability on stable isotopes in precipitation, *J. Geophys. Res.*, 113, D12111,
715 doi:10.1029/2007JD009416, 2008.

716 Schwerdtfeger, W.: *Weather and Climate of the Antarctic*. Elsevier Science Publishers,
717 Amsterdam-London-New York-Tokyo. 262pp, 1984.

718 Seefeldt, M. W., and Cassano, J. J.: An analysis of low-level jets in the greater Ross Ice Shelf
719 region based on numerical simulations. *Mon. Wea. Rev.*, **136**, 4188-4205. doi:
720 10.1175/2007JAMC1442.1, 2008.

721 Seefeldt, M. W., and Cassano, J. J.: A description of the Ross Ice Shelf air stream (RAS)
722 through the use of self-organizing maps (SOMs). *J. Geophys. Res.*, **117**, D09112.
723 doi:10.1029/2011JD016857, 2012.

724 Simmonds, I., Keay, K., and Lim, E.: Synoptic activity in the seas around Antarctica. *Mon.*
725 *Wea. Rev.*, 131, 272-288, 2002.

726 Sinclair, M. R.: Record-high temperatures in the Antarctic – A synoptic case study, *Mon. Wea.*
727 *Rev.*, 109, 2234- 2242, 1981.

728 Skamarock, W. C., Klemp, J. B., Dudhia, J., Gill, D. O., Barker, D. M., Duda, M. G., Huang,
729 X., Wang, W., and Powers, J. G.: A description of the Advanced Research WRF Version 3,
730 NCAR/TN 475+STR, 125 pp., Nat. Cent. for Atmos. Res., Boulder, Co, 2008.

731 Stenni, B., Masson-Delmotte, V., Johnsen, S., Jouzel, J., Longinelli, A., Monnin, E.,
732 Roethlisberger, R., and Selmo, E.: An Oceanic Cold Reversal During the Last Deglaciation,
733 *Science*, 293, 2074-2077, 2001.

734 Stenni, B., Masson-Delmotte, V., Selmo, E., Oerter, H., Meyer, H., Roethlisberger, R., Jouzel,
735 J., Cattani, O., Falourd, S., Fischer, H., Hoffmann, G., Iacumin, P., Johnsen, S. F., Minster, B.,

736 and Udisti, R.: The deuterium excess records of EPICA Dome C and Dronning Maud Land
737 ice cores (East Antarctica), *Quat. Sci. Rev.*, 29, 146-159, 2010.

738 Steen-Larsen, H. C. , S. J. Johnson, S. J., Masson-Delmotte, V., Stenni, B., Risi, C.,
739 Sodemann, H., Balslev-Clausen, D., Blunier, T., Dahl-Jensen, D., Ellehøy, M. D., Falourd, S.,
740 Grindsted, A., Gkinis, V., Jouzel, J., Popp, T., Sheldon, S., Simonsen, S. B., Sjolte, J.,
741 Steffensen, J. P., Sperlich, P., Sveinbjörnsdottir, A. E., Vinther, B. M., White, J. W. C.:
742 Continuous monitoring of summer surface water vapor isotopic composition above the
743 Greenland Ice Sheet, *Atmos. Chem. Phys.*, 13, 4815-4828, 2013.

744 Suzuki, K., Yamanouchi, T., and Motoyama, H.: Moisture transport to Syowa and Dome Fuji
745 stations in Antarctica, *J. Geophys. Res.*, 113, D24 114, doi:10.1029/2008JD009794, 2008.

746 Thompson, D. W. J., and J. M. Wallace: Annular modes in the extratropical circulation. Part I:
747 Month-to-month variability, *J. Climate*, 13, 1000-1016.

748 Trenberth, K. E., and Mo, K. C.: Blocking in the Southern Hemisphere, *Mon. Weather Rev.*,
749 133, 38-53, 1985.

750 Van Loon, H.: The half-yearly oscillation in middle and high southern latitudes and the
751 coreless winter. *J. Atmos. Sci.*, 24, 472-486, 1967.

752 Van Loon, H., and Jenne, R. L., The zonal harmonic standing waves in the Southern
753 Hemisphere, *J. Geophys. Res.*, 77, 992-1003, 1972.

754 Winkelmann, R., Levermann, A., Martin, M. A., and Frieler, K.: Increased future ice
755 discharge from Antarctica owing to higher snowfall. *Nature*, 492, 239-242, 2012.

756

757

758

759

760

761

762

763 **Figure Captions**

764

765 **Fig. 1**

766 Map of Antarctica indicating Dome C and other important deep-drilling sites in Antarctica

767

768 **Fig. 2**

769 AMPS domains used for model output analysis in this study

770

771 **Fig. 3**

772 a) Mean monthly temperatures for 2009 and 2010 at Dome C AWS

773 b) Daily precipitation and daily mean temperature at Dome C for 2009 and 2010

774

775 **Fig. 4**

776 Monthly precipitation at Dome C a) 2009 and b) 2010, distinguishing three different types of
777 precipitation: diamond dust, hoar frost, and snowfall

778 Relative frequency of diamond dust, hoar frost, and snowfall for c) 2009 and d) 2010

779 The types were determined from photos of the crystals on the platforms by the Avalanche
780 Research Institute, Arabba, Italy.

781

782 **Fig. 5**

783 a) 500hPa geopotential height from AMPS archive data (Domain 1) 13.9.2009 00Z

784 (The axis of the upper-level ridge mentioned in the text is marked by a bold black line.)

785 b) 24h-precipitation from AMPS 13.9. 2009 00GMT to 24 GMT

786

787 **Fig. 6**

788 Example for synoptic situation, during which precipitation is observed at Dome C, but not
789 forecast by WRF in AMPS.

790 a) 500 hPa geopotential height, Domain 2.

791 b) 24h-precipitation total (mm) from AMPS

792

793 **Fig. 7**

794 Mean July- 500hPa geopotential height based on AMPS archive model output for 2009 and
795 2010.

796

797 **Fig. 8**

798 Mean monthly SAM index for 2009 and 2010 (after Marshall, 2003).

799

800 **Fig. 9**

801 a) Monthly mean Zonal Wave Number 3 (ZW3) index for 2009-2010

802 b) July 2009 500hPa geopotential height anomaly: Mean July 2009 height minus long-term
803 zonal mean height

804 c) July 2010 500hPa geopotential height anomaly: Mean July 2009 height minus long-term
805 zonal mean height

806

807

808

809

810

811

812 **Fig. 1**

813

814

815

816

817

818

819

820

821

822

823

824

825

826

827

828

829

830

831

832

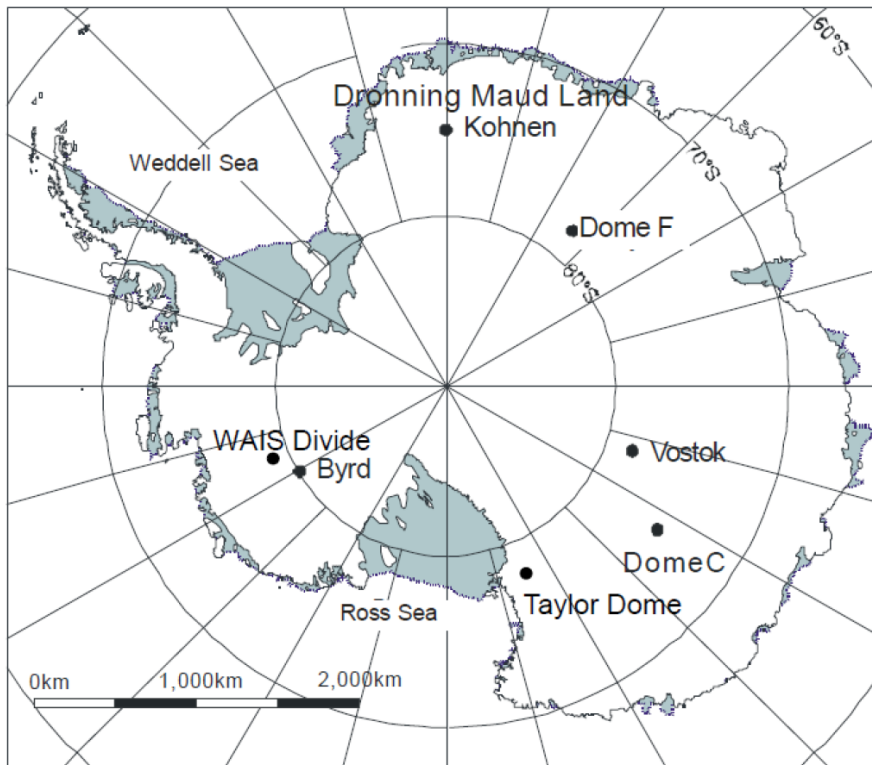
833

834

835

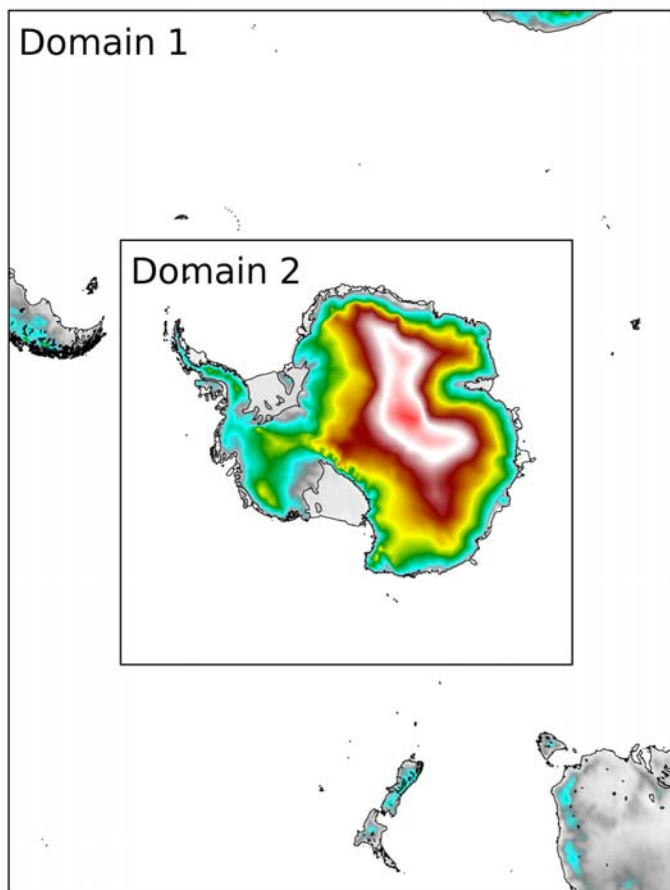
836

837



838 **Fig. 2**

839



840

841

842

843

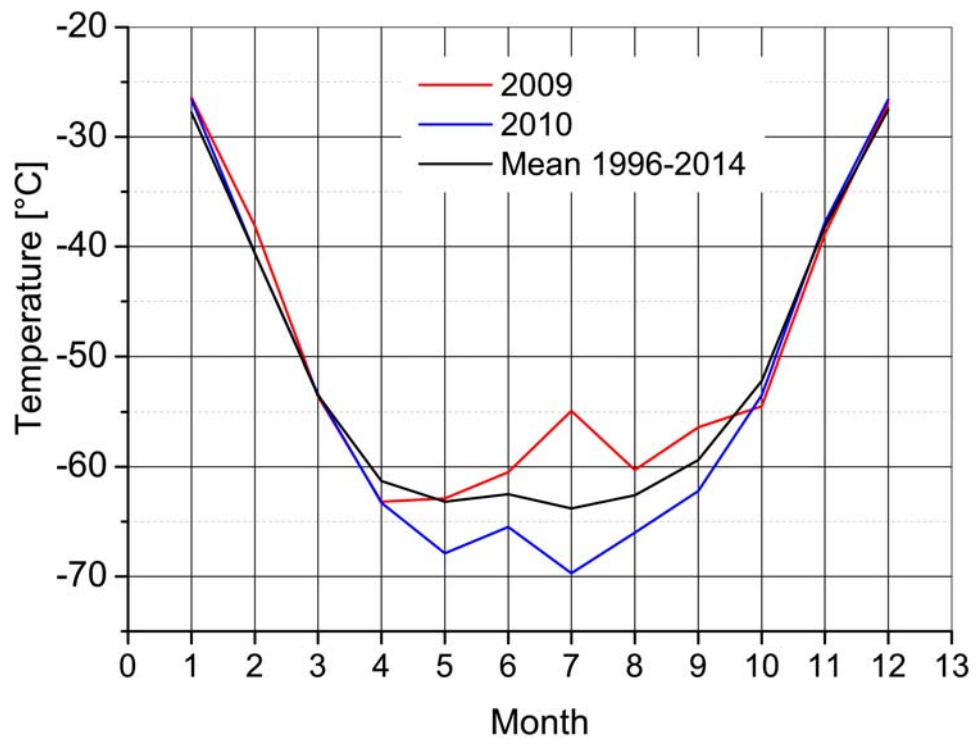
844

845

846 Fig. 3

847

848 a)



849

850

851

852

853

854

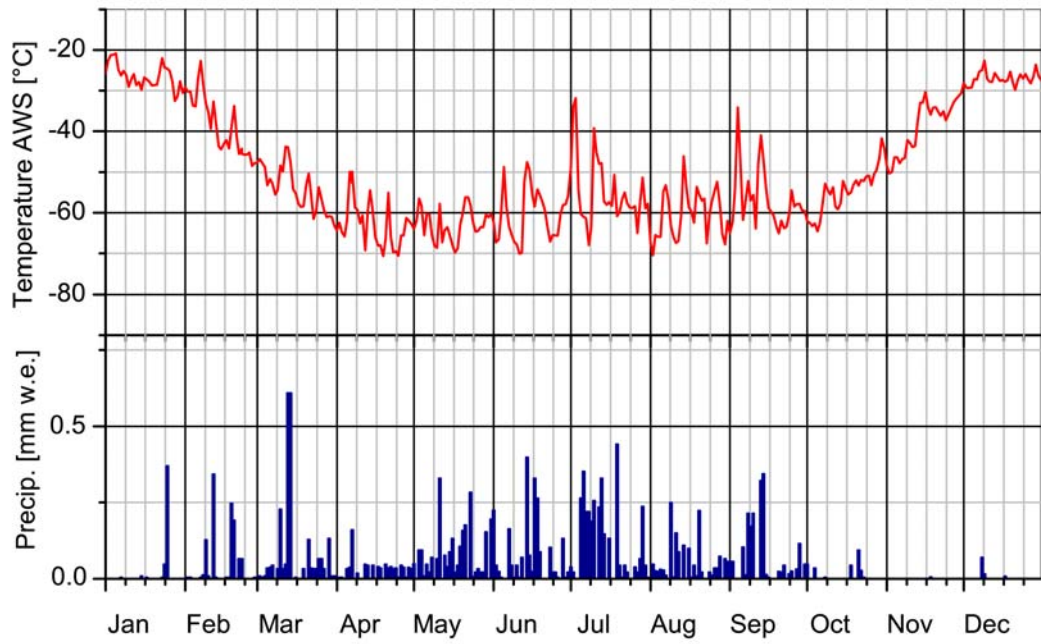
855

856

857

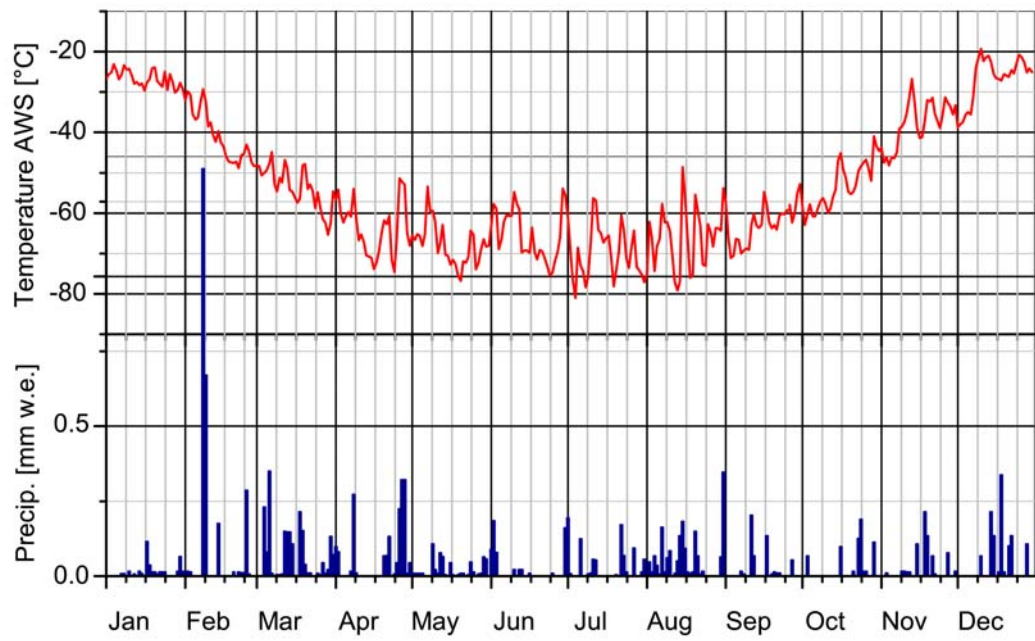
858 b)

859 2009



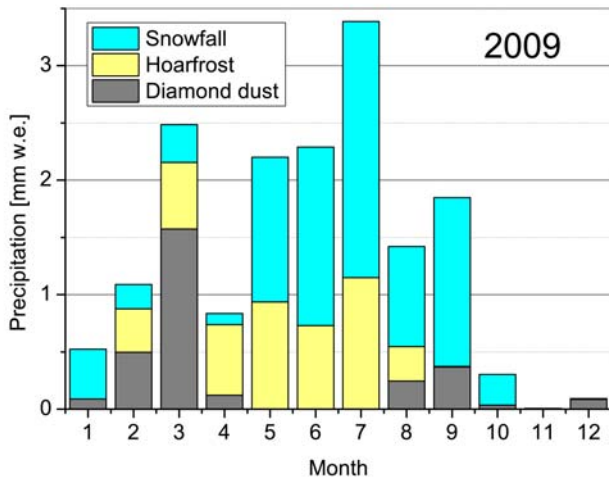
860 2010

861

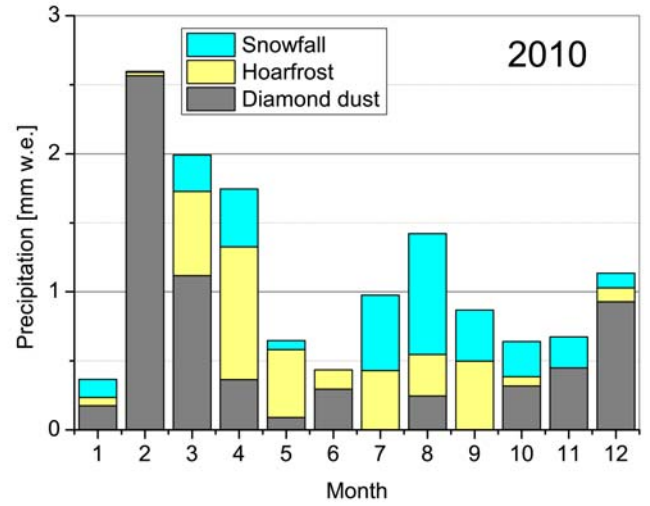


862 **Fig. 4**

863 a)



b)



864

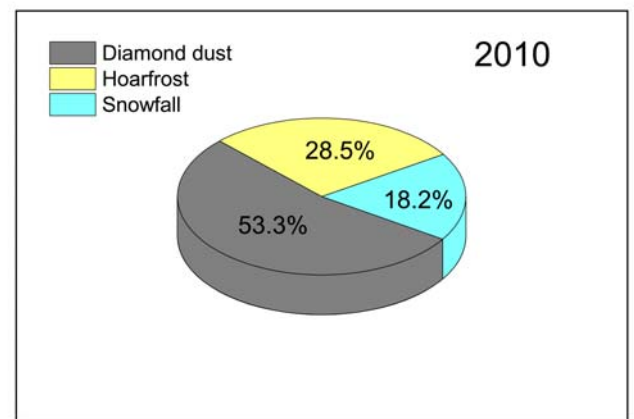
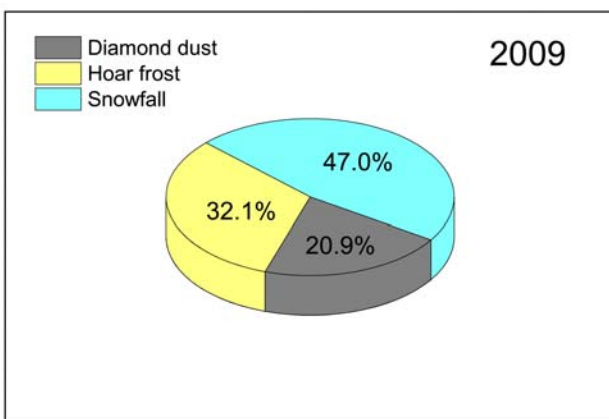
865

866 c)

867

868

d)



869

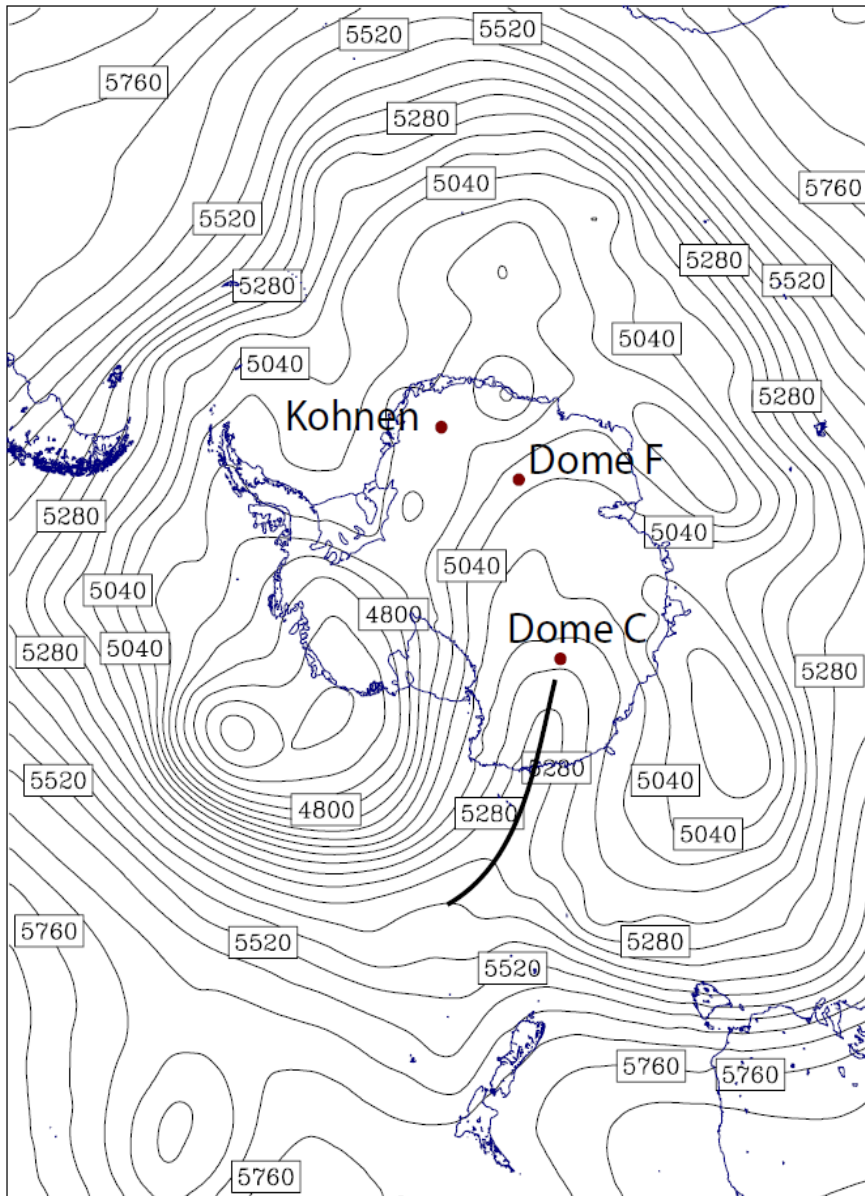
870

871

872 Fig. 5

873 a)

874



890

891

892

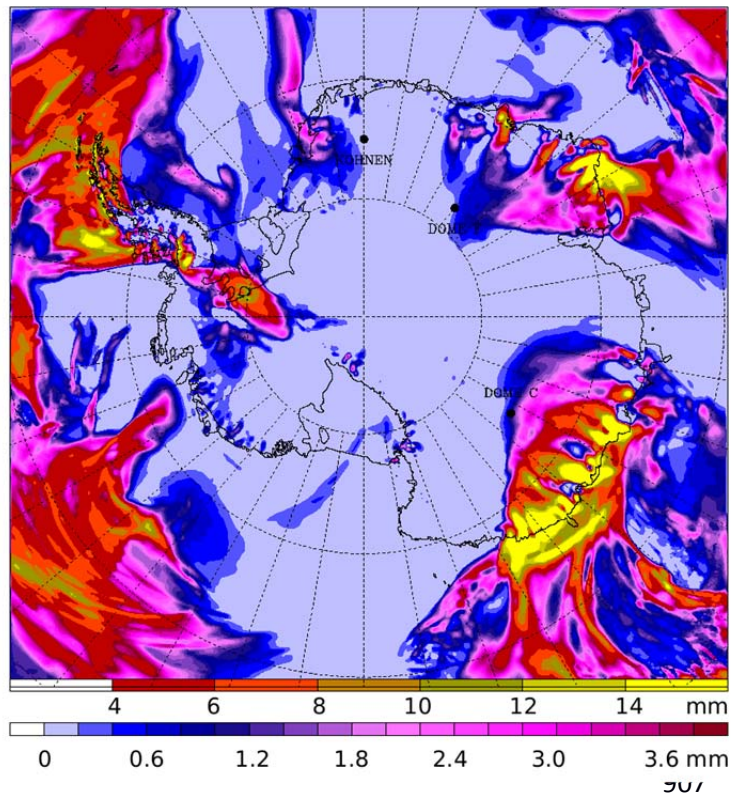
893

894

895

896 b)

897



908

909

910

911

912

913

914

915

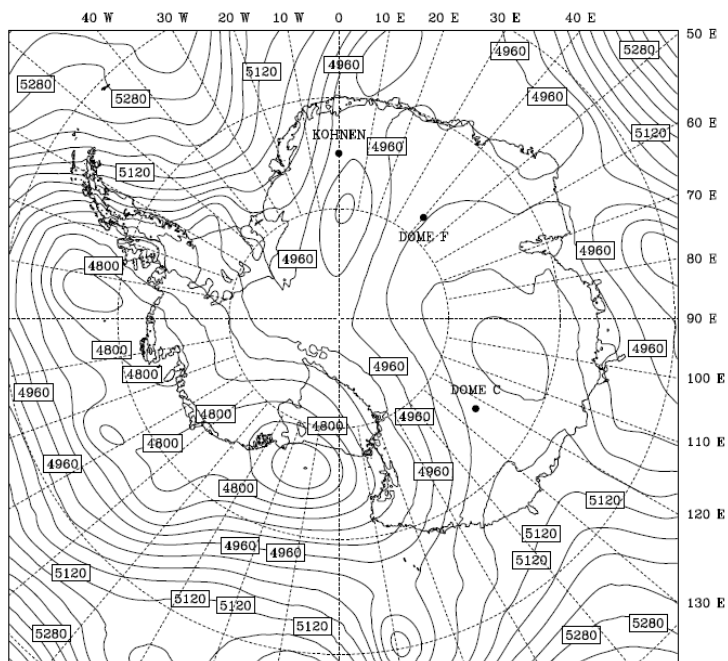
916

917

918 Fig. 6

919 a)

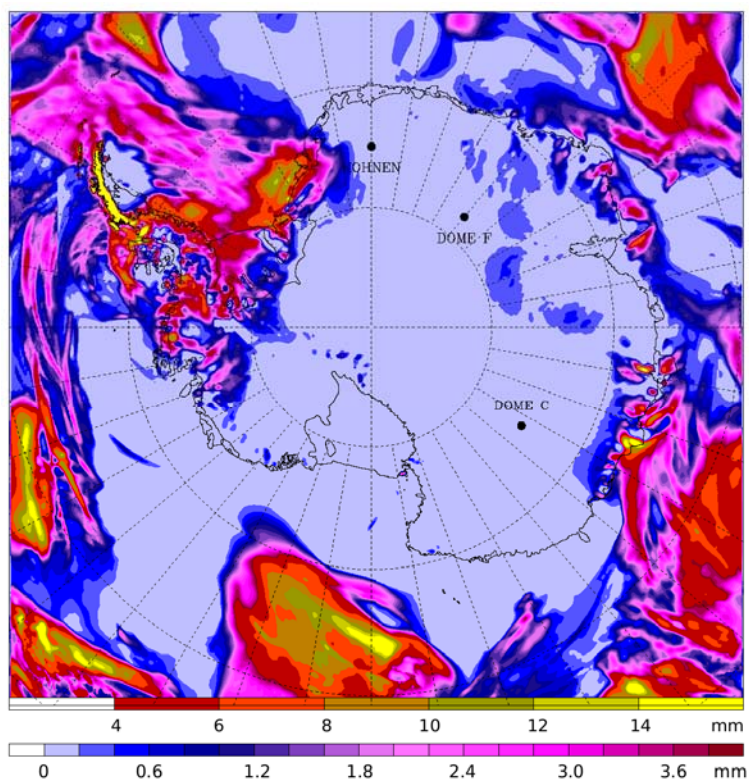
920



930

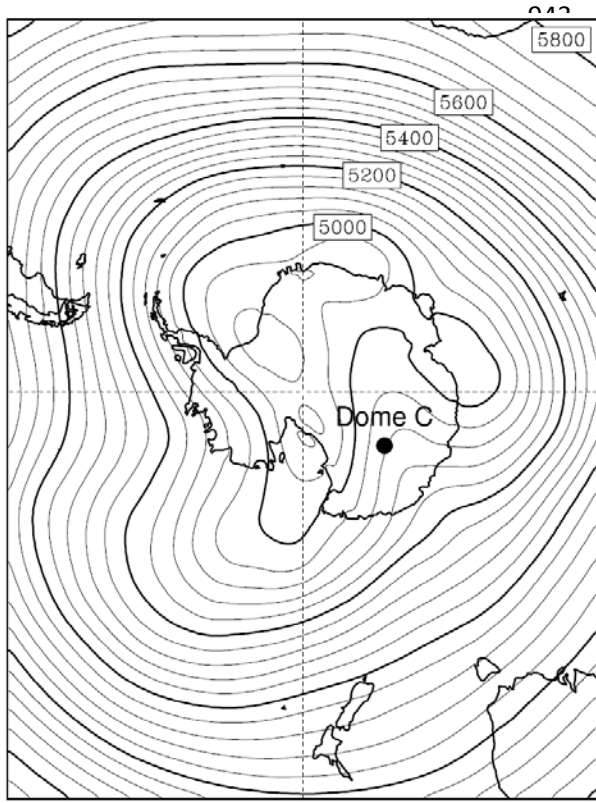
931 b)

932

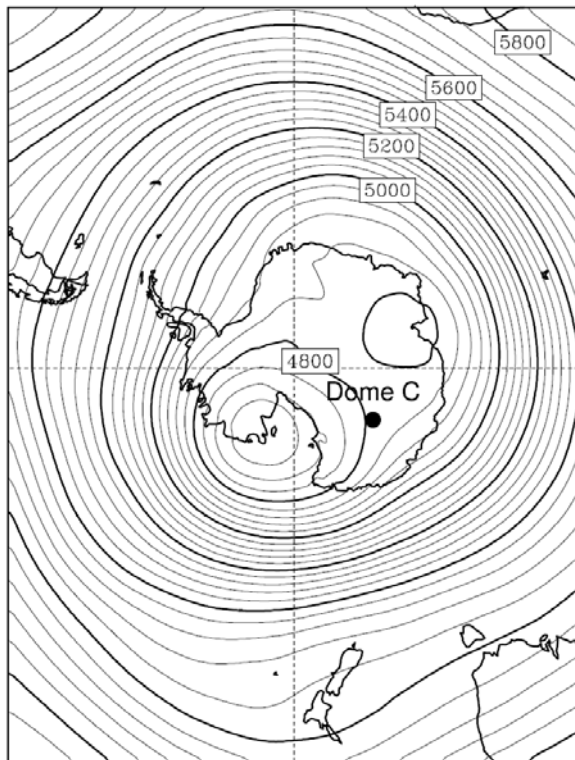


941 **Fig. 7**

942 a) July 2009



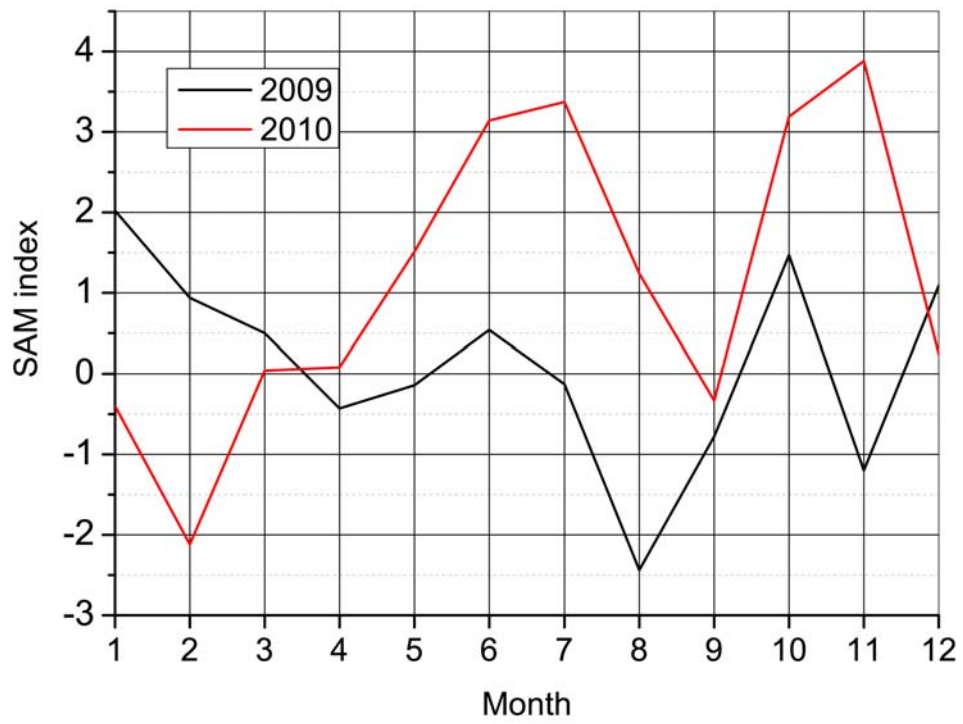
953 b) July 2010



964 **Fig. 8**

965

966



967

968

969

970

971

972

973

974

975

976 **Fig. 9**

977 a)

978

979

980

981

982

983

984

985

986

987

988

989

990

991

992

993

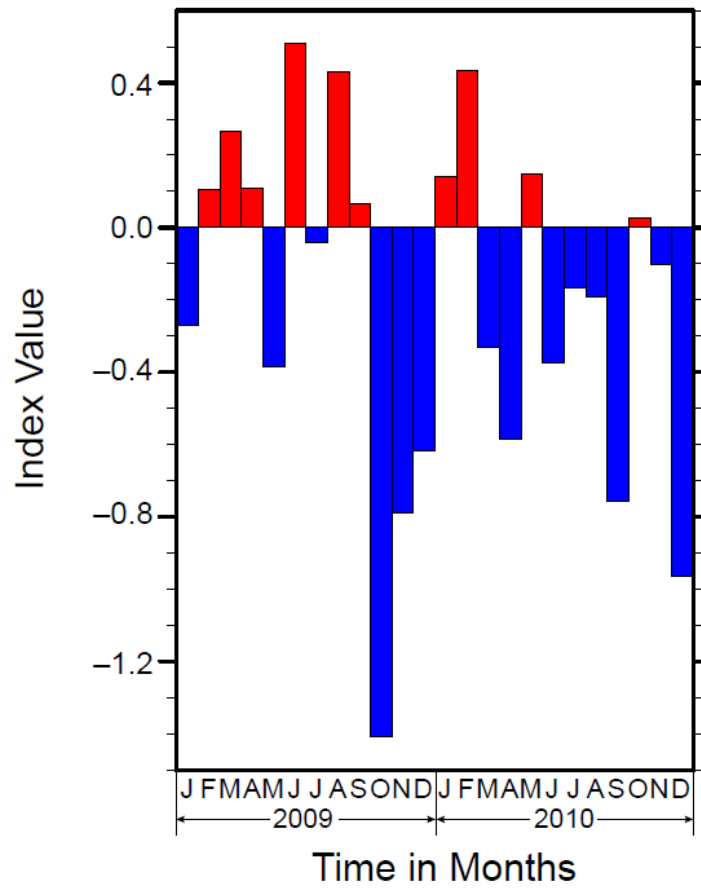
994

995

996

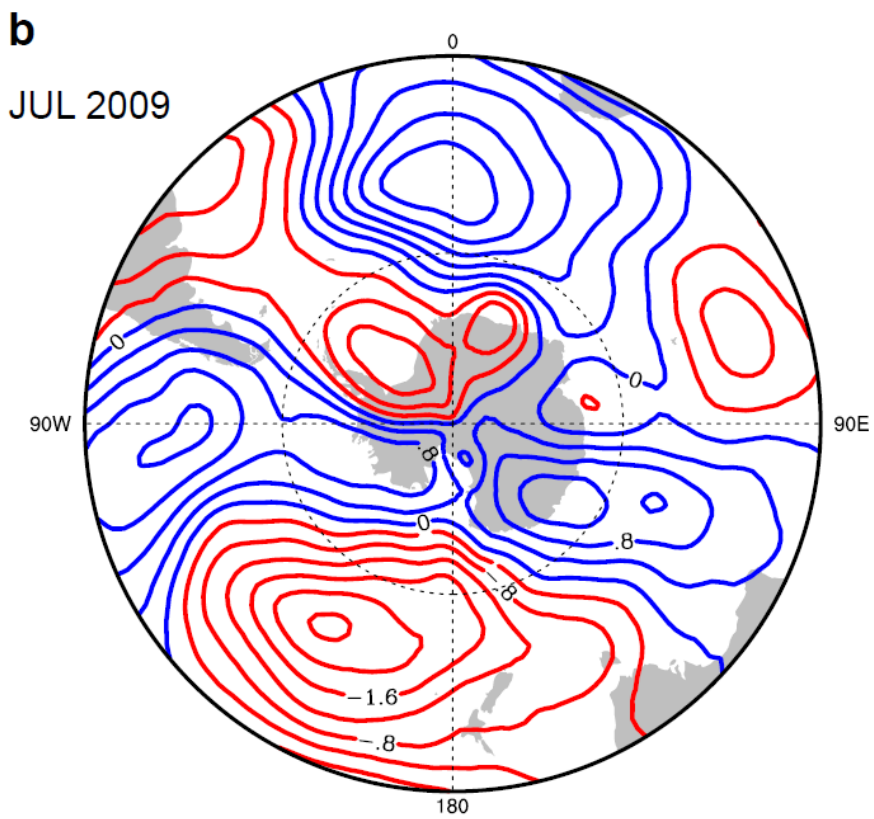
997

998



999 b) 500hPa geopotential height: mean July 2009 minus long-term zonal mean

1000



1011 c) 500hPa geopotential height: mean July 2010 minus long-term zonal mean

1012

